10-26-2021

Radiocarbon Analyses Quantify Peat Carbon Losses With Increasing Temperature in a Whole Ecosystem Warming Experiment

Rachel M. Wilson

Natalie A. Griffiths

Ate Visser

Karis J. McFarlane

Stephen D. Sebestyen

See next page for additional authors

Radiocarbon Analyses Quantify Peat Carbon Losses With Increasing Temperature in a Whole Ecosystem Warming Experiment

Comments

This article was originally published in *Journal of Geophysical Research: Biogeosciences*, volume 126, in 2021. https://doi.org/10.1029/2021JG006511

Creative Commons License

Copyright

Authors

Rachel M. Wilson, Natalie A. Griffiths, Ate Visser, Karis J. McFarlane, Stephen D. Sebestyen, Keith C. Oleheiser, Samantha Bosman, Anya M. Hopple, Malak M. Tfaily, Randall K. Kolka, Paul J. Hanson, Joel E. Kostka, Scott D. Bridgham, Jason K. Keller, and Jeffrey P. Chanton

ADVANCING EARTH AND SPACE SCIENCE

JGR Biogeosciences

RESEARCH ARTICLE
10.1029/2021JG006511

Radiocarbon Analyses Quantify Peat Carbon Losses With Increasing Temperature in a Whole Ecosystem Warming Experiment

Rachel M. Wilson[1], Natalie A. Griffiths[2], Ate Visser[3], Karis J. McFarlane[3], Stephen D. Sebestyen[4], Keith C. Oleheiser[2], Samantha Bosman[1], Anya M. Hopple[5,6], Malak M. Tfaily[7], Randall K. Kolka[4], Paul J. Hanson[2], Joel E. Kostka[8], Scott D. Bridgham[5], Jason K. Keller[9], and Jeffrey P. Chanton[1]

[1]Department of Earth Ocean and Atmospheric Science, Florida State University, Tallahassee, FL, USA, [2]Oak Ridge National Laboratory, Environmental Sciences Division, Oak Ridge, TN, USA, [3]Lawrence Livermore National Laboratory, Livermore, CA, USA, [4]US Department of Agriculture Forest Service, Northern Research Station, Grand Rapids, MN, USA, [5]Institute of Ecology and Evolution, University of Oregon, Eugene, OR, USA, [6]Pacific Northwest National Laboratory, Smithsonian Environmental Research Center, Edgewater, MD, USA, [7]Department of Environmental Science, University of Arizona, Tucson, AZ, USA, [8]School of Biological Sciences, Georgia Institute of Technology, Atlanta, GA, USA, [9]Schmid College of Science and Technology, Biological Sciences, Chapman University, Orange, CA, USA

Key Points:

- Radiocarbon mass balance demonstrates the loss of peat carbon in a peatland ecosystem warming experiment
- Peat carbon losses increased with warming treatment
- Tritium-based analyses calculate approximately 30 cm y^{-1} downward advection of porewater through the top 1 m of peat

Supporting Information:

Supporting Information may be found in the online version of this article.

Correspondence to:

R. M. Wilson,
rmwilson@fsu.edu

Citation:

Wilson, R. M., Griffiths, N. A., Visser, A., McFarlane, K. J., Sebestyen, S. D., Oleheiser, K. C., et al. (2021). Radiocarbon analyses quantify peat carbon losses with increasing temperature in a whole ecosystem warming experiment. *Journal of Geophysical Research: Biogeosciences*, *126*, e2021JG006511. https://doi.org/10.1029/2021JG006511

Received 1 JUL 2021
Accepted 19 OCT 2021

Author Contributions:

Conceptualization: Natalie A. Griffiths, Karis J. McFarlane, Stephen D. Sebestyen, Malak M. Tfaily, Randall K. Kolka, Paul J. Hanson, Joel E. Kostka, Scott D. Bridgham, Jason K. Keller, Jeffrey P. Chanton
Data curation: Ate Visser
Formal analysis: Rachel M. Wilson, Natalie A. Griffiths, Ate Visser, Karis J. McFarlane, Stephen D. Sebestyen, Keith C. Oleheiser, Samantha Bosman, Anya M. Hopple, Malak M. Tfaily, Randall K. Kolka, Paul J. Hanson, Joel E. Kostka,

Abstract Climate warming is expected to accelerate peatland degradation and release rates of carbon dioxide (CO_2) and methane (CH_4). Spruce and Peatlands Responses Under Changing Environments is an ecosystem-scale climate manipulation experiment, designed to examine peatland ecosystem response to climate forcings. We examined whether heating up to +9 °C to 3 m-deep in a peat bog over a 7-year period led to higher C turnover and CO_2 and CH_4 emissions, by measuring ^{14}C of solid peat, dissolved organic carbon (DOC), CH_4, and dissolved CO_2 (DIC). DOC, a major substrate for heterotrophic respiration, increased significantly with warming. There was no 7-year trend in the $DI^{14}C$ of the ambient plots which remained similar to their $DO^{14}C$. At +6.75 °C and +9 °C, the ^{14}C of DIC, a product of microbial respiration, initially resembled ambient plots but became more depleted over 7 years of warming. We attributed the shifts in $DI^{14}C$ to the increasing importance of solid phase peat as a substrate for microbial respiration and quantified this shift via the radiocarbon mass balance. The mass-balance model revealed increases in peat-supported respiration of the catotelm depths in heated plots over time and relative to ambient enclosures, from a baseline of 20%–25% in ambient enclosures, to 35%–40% in the heated plots. We find that warming stimulates microorganisms to respire ancient peat C, deposited under prior climate (cooler) conditions. This apparent destabilization of the large peat C reservoir has implications for peatland-climate feedbacks especially if the balance of the peatland is tipped from net C sink to C source.

Plain Language Summary Since the end of the last glacial period, about 20 thousand years ago, peatlands have taken up carbon and now store an amount nearly equivalent to the quantity in the atmosphere. Microorganisms consume and respire that peat C releasing it back to the atmosphere as CO_2 and CH_4. Until now, many studies have shown that microorganisms prefer to consume the most recently fixed carbon and that the deeply buried ancient peat carbon reservoir is relatively stable. However, climate warming is expected to upset that balance. The Spruce and Peatlands Responses Under Changing Environments is large-scale experimental warming of a Minnesota peatland designed to study these effects. We conducted radiocarbon analysis of the peat and the microbially produced CO_2 and dissolved organic carbon in ambient and heated areas of the peatland and show that at warmer temperatures more of the ancient peat carbon is being mobilized and respired to CO_2. This is troubling as it signifies a positive feedback loop wherein warming stimulates peat to produce more CO_2 which further exacerbates climate change.

1. Introduction

Peatlands cover only a small fraction of the Earth's surface (3%), yet store more than 15%–30% of terrestrial carbon (C) stocks (Holden, 2005; Nichols & Peteet,, 2019). Although estimates of C accumulation in

Scott D. Bridgham, Jason K. Keller, Jeffrey P. Chanton
Funding acquisition: Randall K. Kolka, Paul J. Hanson, Joel E. Kostka, Scott D. Bridgham, Jason K. Keller, Jeffrey P. Chanton
Investigation: Rachel M. Wilson, Natalie A. Griffiths, Ate Visser, Keith C. Oleheiser, Samantha Bosman, Anya M. Hopple, Malak M. Tfaily, Randall K. Kolka, Paul J. Hanson, Joel E. Kostka, Scott D. Bridgham, Jason K. Keller, Jeffrey P. Chanton
Methodology: Natalie A. Griffiths, Ate Visser, Karis J. McFarlane, Stephen D. Sebestyen, Jeffrey P. Chanton
Project Administration: Randall K. Kolka, Paul J. Hanson, Joel E. Kostka, Scott D. Bridgham, Jason K. Keller, Jeffrey P. Chanton
Resources: Paul J. Hanson, Jeffrey P. Chanton
Supervision: Stephen D. Sebestyen, Malak M. Tfaily, Randall K. Kolka, Paul J. Hanson, Joel E. Kostka, Scott D. Bridgham, Jason K. Keller, Jeffrey P. Chanton
Validation: Karis J. McFarlane
Visualization: Rachel M. Wilson, Ate Visser
Writing – original draft: Rachel M. Wilson
Writing – review & editing: Natalie A. Griffiths, Ate Visser, Karis J. McFarlane, Stephen D. Sebestyen, Samantha Bosman, Anya M. Hopple, Malak M. Tfaily, Randall K. Kolka, Paul J. Hanson, Joel E. Kostka, Scott D. Bridgham, Jeffrey P. Chanton

northern peatlands vary widely (Yu, 2012), the sheer existence of large peat reservoirs points to their function as C sinks. More than 90% of this C resides in peatlands in northern latitudes (Yu et al., 2010), where climate warming is expected to be intensified relative to lower latitudes (Collins et al., 2013). Because cold temperatures are believed to contribute to the slow decomposition of peat C (Limpens et al., 2008), climate warming could accelerate C losses in the form of carbon dioxide (CO_2) and methane (CH_4), which are two important greenhouse gases. Further, evidence suggests that warming will shift greenhouse gas production toward a higher proportion of CH_4 relative to CO_2 (Hopple et al., 2020; Wilson et al., 2016, 2021). Because of the higher global warming potential of CH_4 relative to CO_2 (Neubauer & Megonigal, 2015; Ramaswamy et al., 2001), such a shift could intensify peatland-climate feedbacks. Further, because of the differential global warming potential of CH_4 relative to CO_2, declining CO_2:CH_4 ratios could create the situation where a peatland remains a net C sink, but increases in net radiative forcing (Wilson et al., 2017).

The net C balance of a peatland reflects the balance between primary production and ecosystem respiration which includes microbial production of CO_2 and CH_4. Dominant vegetation type (e.g., moss vs. sedge), hydrologic conditions, nutrient availability, and pH are among the factors contributing to the high variability in C balance among peatlands. Such variability can occur spatially across similar peatlands spanning small geographic scales (e.g., Wilson et al., 2017; Zalman et al., 2018) or interannually (e.g., Euskirchen et al., 2014). The Spruce and Peatlands Response Under Changing Environments (SPRUCE) experiment is a uniquely designed ecosystem-scale, decade-long climate manipulation (described in detail in Hanson et al., 2017) to explore peatland C source/sink capacity changes in response to warming and higher levels of atmospheric CO_2.

Warming can stimulate organic matter decomposition in northern peatlands through thermal kinetic effects or by increasing the efficiency of the microbial community (Kolton et al., 2019). However, this response can also be (partially) offset by concurrent increases in plant productivity with warming (Bjorkman et al., 2018; Burke et al., 2017; Elmendorf et al., 2012). Calculations of net C balance in peatlands are complicated by high spatial and temporal variability in individual components (Griffiths et al., 2017). Many sources of C cycle variability are attributed to surface ecosystem processes, such as changing phenology, variability in annual precipitation, water table variation, fire losses, etc. Such processes are likely to have the greatest influence on the surface and diminishing effects with depth. For example, water table variations likely have little influence on the catotelm (i.e., permanently saturated peat underlying a surficial acrotelm layer) C dynamics. Thus, we expect variation in deep C losses to be less variable across both space and time than calculations of net C balance. The balance is further complicated by the potential for priming of decomposition in which previously stable C becomes susceptible to decomposition in conjunction with increasing supply of more labile substrates (Blagodatskaya & Kuzyakov, 2008).

Prior to initiation of the SPRUCE warming treatments, the C standing stock from 0 to 2 m deep in the SPRUCE peatland was estimated to be 158 ± 14 kg C m^{-2} and the peatland were estimated to be at near-zero C balance—within the variability of the data (Griffiths et al., 2017). *Sphagnum* mosses were the greatest contributor to net primary production across the bog (Griffiths et al., 2017), but declining *Sphagnum* moss cover with warming (Norby et al., 2019) has contributed to declining C uptake shifting the C balance of the peatland towards a net C source (Hanson et al., 2020). Additionally, CO_2 and CH_4 production has increased with warming (Hanson et al., 2020; Hopple et al., 2020; Wilson et al., 2016) suggesting destabilization of previously stored peat C. Although early results suggest that increased deposition of fresh organic matter (OM) due to warming stimulates decomposition (Wilson et al., 2016, 2021), other analyses suggest that prolonged warming could be mobilizing and decomposing ancient peat, potentially through a priming effect (Hopple et al., 2020) which would amplify soil C losses (Keuper et al., 2020).

Recent results following the first three years of experimental warming suggest that warming resulted in net C loss mostly as a result of increased peat decomposition (Hanson et al., 2020). This result is corroborated by high-precision measurements of peat elevation at SPRUCE using a modified surface elevation table instrument (SET; Boumans & Day, 1993; Cahoon et al., 2002) anchored to the glacial till underlying the bog peat (Hanson et al., 2020). One of the sources of potential error using this approach is the interpretation of what constitutes the surface being measured. This is particularly relevant in peatlands which are covered with pliable mosses and where it is difficult to distinguish actual mass loss from compaction, drying, changes in roots (Thomas & Ridd, 2004), or some combination of these effects. In addition, measurements

of net ecosystem exchange determined from the difference in C uptake by above and belowground net primary production versus C loss from heterotrophic CO_2 and CH_4 efflux and loss of DOC and DIC to surface water outflow further indicated a shift in the system from a C sink to an atmospheric C source (Hanson et al., 2020). To further constrain the changes in the C balance, we used a ^{14}C-based method to analyze the source of respiration products in porewater profiles belowground. We used radiocarbon (^{14}C)-based mass balance to differentiate between recently-fixed DOC and ^{14}C-depleted peat contributions to the respiration products and better constrain SET and C mass balance measurements. We hypothesized that changes in peat elevation are due, at least in part, to loss of peat C. Further, we hypothesized that the magnitude of peat C loss will increase with increasing temperature and over time throughout the warming treatment period. To investigate the C balance of a warming peatland, we modeled C loss from an experimentally warmed peatland and quantified the contribution of old peat to C losses. Applying the model in a depth stratified approach, we identified the zone of greatest CO_2 and CH_4 production and quantified subsurface mass losses of ancient, previously-stored peat C.

2. Materials and Methods

2.1. Site Description

The S1 bog, site of the SPRUCE experiment, is located in northern Minnesota (USA) within the USDA Forest Service Marcell Experimental Forest (N47°30.476'; W93°27.162'). S1 is a perched ombrotrophic bog that receives 787 mm ± 104 mm (s.d.) annual average precipitation and has no apparent input from the surrounding groundwater aquifer (Sebestyen, Funke, & Cotner, 2021). Water table elevation historically varies about 0.5 m per year, from 411.8 to 412.3 m above sea level (Griffiths et al., 2019). The SPRUCE experiment comprises a climate manipulation that includes both warming and elevated atmospheric CO_2 (Hanson et al., 2017). Ten plots (12.8 m diameter) are surrounded by 7 m meter tall enclosures, with the top open for precipitation inputs, atmospheric deposition, and peatland-atmosphere energy and vapor exchange (an illustration of the enclosures is available in Hanson et al., 2017). Corrals extending from 0.3 m above the surface of the peat up to 3–4 m deep into the underlying lake sediment isolate the subsurface peat hydrology from the rest of the S1 bog (Sebestyen & Griffiths, 2016). The experiment is designed such that the 10 randomly selected enclosures are warmed at five levels (+0, +2.25, +4.5, +6.75, +9 °C above the control enclosure). Treatment began with deep peat heating in June of 2014 with an array of vertically installed electric resistance rods (Hanson et al., 2011; Wilson et al., 2016). The following year, whole-ecosystem warming, which included heating of the overlying ambient air began in August 2015 when the aboveground enclosures were completed (Hanson et al., 2017). The third phase of the experiment, elevated air CO_2 (~900 p.p.m.v.) in half of the enclosures, was initiated in June of 2016. Five of the 10 enclosures (including each warming level) are subjected to an elevated air CO_2 concentration (eCO_2) while the other five contain ambient air CO_2. The source of the CO_2 for the eCO_2 treatment is pure CO_2 from a commercial facility with a radiocarbon-dead (−999‰) $^{14}CO_2$ and a depleted $^{13}CO_2$ (−40‰) signature. When mixed with ambient air to achieve about 900 p.p.m.v. during the growing season, the resulting mean measured isotopic values of the air in the plots were $^{14}C = -523‰ \pm 32$ (s.d.) and $\delta^{13}C = -25.7‰ \pm 1.0‰$ (s.d.). In the ambient plots, $^{14}C = -33.2 \pm 26.3‰$ and $\delta^{13}CO_2 = -8.3‰ \pm 0.9‰$ (s.d.). Given the uncertainty introduced into the isotopic signal of the CO_2, we focused on plots that did not receive elevated CO_2. Treatments examined include +9 °C (Plot 17), +6.75 °C (Plot 8), +4.5 °C (Plot 13), +2.25 °C (Plot 20) enclosures, an unheated enclosure (Plot 6) and an unheated, unchambered control site (T3F) on the same transect as Plot 8.

2.2. Sample Collection

Porewater was collected from a set of piezometers located within each treatment enclosure and at the unheated control location up to four times annually from June 2014 through August 2020. Each piezometer consists of a 2.5 cm diameter poly vinyl chloride (PVC) pipe with a screen mesh bottom installed to specified depths below the peat hollow surface: 25 cm, 50 cm, 75 cm, 100 cm, 150 cm, and 200 cm. Piezometers were covered, but not sealed, when not being actively sampled. Prior to porewater sampling, the piezometers were pumped dry and then allowed to recharge over 12 hr. Given the small surface area of the pipes, the diffusion of gases into and out of the porewater is generally assumed to be negligible over the 12-hr recharge period. This assumption is supported by finding near or slightly above saturation concentrations of gases

in the deep porewater. Porewater was sampled from each piezometer using a peristaltic pump attached to a syringe. Surface water samples (10 cm) were collected using perforated stainless-steel tubes that were inserted into the peat to 10 cm or the top of the water table, whichever was shallowest. Porewater samples were measured for DOC and DIC concentrations, as well as stable ^{13}C and radiocarbon (^{14}C) isotopic composition. Additionally, each enclosure has an outlet that allows water to passive lateral drainage from the top 25 cm, which to mimics near-surface drainage that dominates the annual movement of water to the outlet stream (Romanov 1961; Sebestyen & Griffiths, 2016; Verry, Brooks, et al., 2011). We measured DIC concentrations and ^{13}C isotopes in porewater collected from each of these "outflows" monthly June-December of 2016, and March-November of 2017 when there was flow (Sebestyen, Griffiths, et al., 2021). We also collected outflow water and here report DOC concentrations for August in each year of 2016–2019.

2.3. Dissolved CO_2 and CH_4 Analyses

All water samples were immediately injected into septum-sealed evacuated glass vials. A 1 mL aliquot of 10% phosphoric acid was added to each vial to preserve the samples and ensure that all DIC was in the form of dissolved CO_2 (i.e., not bicarbonate or carbonate). Porewater CO_2 and CH_4 concentrations and isotopes were analyzed simultaneously via headspace analysis using a Finnigan Mat Delta V Isotope Ratio Mass Spectrometer coupled to a gas chromatograph (Merritt et al., 1995). The analytical uncertainty based on repeated measurements of a standard was <0.15‰ for $\delta^{13}CO_2$ and $\delta^{13}CH_4$ and <5% for CO_2 and CH_4 concentrations. To prepare samples for CH_4 and dissolved CO_2 radiocarbon analyses, helium was used to strip the gases from the vials. The CO_2 and CH_4 were cryogenically separated. The CO_2 was then flame-sealed in a 6 mm Pyrex tube using a vacuum line. The CH_4 was converted to CO_2 via combustion at 580 °C for 18 hr, followed by cryogenic purification, and then was flame sealed in a 6 mm Pyrex tube under vacuum. The 6 mm tubes for $\Delta^{14}C$ analysis were sent to the National Ocean Sciences Accelerator Mass Spectrometry Facility (NOSAMS) and the Lawrence Livermore National Laboratory (LLNL). All radiocarbon values were corrected for biological mass-dependent fractionation using $\delta^{13}C$.

2.4. Dissolved Organic Carbon Analyses

Following gas analysis, the concentration of DOC in porewater samples was measured by high-temperature catalytic oxidation using a Shimadzu Total Organic Carbon analyzer equipped with a non-dispersive infrared detector. Samples were analyzed in triplicate with a coefficient of variance <2%. To prepare samples for DOC radiocarbon (^{14}C) analysis, the porewater was freeze-dried in pre-combusted 9 mm Pyrex tubes. Oxidizing agents such as, cupric oxide, copper shots, and silver, were added to each tube which was then evacuated and flame sealed. To convert the organic C to CO_2, the sealed tubes were combusted at 580 °C for 18 h. The resulting CO_2 was purified cryogenically and sealed into 6 mm Pyrex tubes. Sample was sent to NOSAMS and LLNL for ^{14}C analyses. All radiocarbon values were corrected for biological mass-dependent fractionation using the $\delta^{13}C$.

2.5. Tritium and ^{3}Helium Analyses

Tritium (^3H) was used as a tracer to measure porewater advection rates downward through the peat profile. Porewater samples for tritium analyses were collected from 5-cm diameter PVC pipe wells permanently installed in the enclosures similar to the smaller piezometers described earlier. Each well had a 10-cm long screened section starting at 0, 30, 50, 100, 200, or 300 cm depth. Samples were collected in three of the experimental enclosures: ambient (Plot 6), +4.5 °C (Plot 13), and a +9 °C (Plot 17) in June of 2014 and one year later in June 2015. Precipitation samples for tritium analyses were composited from three funnel-type precipitation collectors (Sebestyen et al., 2020), one along each of the same transects that the experimental enclosures lie in the S1 bog. Ten precipitation samples were collected between 5 March and 24 August 2015. Porewater samples for helium analyses were collected into crimped copper tubes using a peristaltic pump, from the 2.5 cm piezometers in the same plots described above.

Water samples were analyzed for low-level tritium by ^{3}Helium accumulation and noble gas mass spectrometry at LLNL (Surano et al., 1992; Visser et al., 2013). Tritium concentrations are reported in pico-Curies per liter water (pCi L^{-1}). The measurement uncertainty was calculated for each measurement by propagating

the uncertainty associated with signal noise, instrument background, and calibration of the instrument against a NIST standard. We averaged ^{3}H concentrations and helium results across all plots and sample dates to reduce variability. ^{3}Helium samples were analyzed at LLNL by noble gas mass spectrometry for the dissolved helium concentration and isotope ratio, as well as the concentrations of neon, argon, krypton, and xenon (Visser et al., 2016).

2.6. Modeling

To determine the fraction of peat contributing to microbial respiration, we conducted a two end-member mixing model using the radiocarbon content of each potential substrate pool as the tracer. The two end-members under consideration were (a) recently-fixed DOC which has been shown to contribute substantially to heterotrophic respiration in numerous other peatland studies (Chasar et al., 2000; Chanton et al., 2008; Hopple et al., 2019; Tfaily et al., 2014; Wilson et al., 2016) and (b) the peat at the depth the DIC is produced. The mass balance was formulated as:

$$\Delta^{14}C_{DIC} = \Delta^{14}C_{DOC} \times F_{DOC} + \Delta^{14}C_{peat} \times F_{peat} \quad (1)$$

$$F_{DOC} + F_{peat} = 1 \quad (2)$$

where F_{DOC} and F_{peat} are the fraction contributions of DOC and peat respectively. For the peat radiocarbon we used the values for SPRUCE peat reported by McFarlane et al. (2018) all collected in 2012 before any treatments were initiated at the site. It seemed likely that recently fixed (presumably more labile) DOC with a higher radiocarbon value was being preferentially consumed with depth. This assumption is supported by the observation that $\Delta^{14}C_{DIC}$ is sometimes less negative than the $\Delta^{14}C_{DOC}$ at a given depth (Figure S1 in Supporting Information S1). In these cases, a mass balance based on the $\Delta^{14}C_{DOC}$ at the depth where the DIC is produced would result in implausible (e.g., $F_{peat} << 0\%$) mass balance values. We reasoned therefore that using the $\Delta^{14}C_{DOC}$ only from the surface peat in all the mass balance calculations would solve this problem and provide us with a conservative estimate of the F_{peat}. The validity of this approach is supported by a more recent analysis in 2020 of the peat ^{14}C which showed that the surface peat ^{14}C is less positive in 2019 (compared to 2012) consistent with higher inputs of more recently fixed, less positive, post-bomb-peak C to the surface (P.J. Hanson and K.J. McFarlane, *unpublished data*) that is rapidly advecting downward through the peat profile.

2.7. Estimating Advection Rates

We estimated downward water advection rates from changes in porewater natural abundance tritium (^{3}H) concentrations with depth. Tritium decays to ^{3}Helium with a half-life of 12.32 years. The age of the porewater at a given depth is calculated from the activity of the porewater at that depth (A_{sample}) relative to the activity of precipitation ($A_{initial}$):

$$Age = \frac{\ln\left(\frac{A_{initial}}{A_{sample}}\right)}{\lambda} \quad (3)$$

decay constant of ^{3}H (λ) = 0.05626 a^{-1}

The ratio of tritium and the decay product, ^{3}Helium, provides an independent estimate of the subsurface travel time. However, loss of tritiogenic ^{3}Helium across the water-atmosphere interface can limit the application in near-surface pore waters. To calculate the ^{3}H/^{3}He age, the initial concentration in Equation 3 is replaced by the sum of tritium and tritiogenic helium:

$$Age = \frac{\ln\left(1 + \frac{^3He_s^*}{A_{sample}}\right)}{\lambda}, \quad (4)$$

where $^3He_s*$ is the "tritiogenic" helium produced by ^{3}H decay in the sampled porewater, expressed as pCi L^{-1} of decayed tritium. The tritiogenic ^{3}Helium was calculated from the concentrations and isotope ratios of dissolved helium:

$$^3He_s* = {}^3He_s - {}^3He_a = \left(R_s - \alpha R_a\right) \times {}^4He_s, \tag{5}$$

where ^3He_a and ^3He_s are the atmospheric and sampled ^{3}Helium concentrations, R_a and R_s are the atmospheric and sampled helium isotope ratios (respectively), α is the equilibrium fractionation factor for ^{3}Helium dissolution in water ($\alpha = 0.983$) and ^4He_s is the dissolved ^{4}Helium concentration. This equation separates the tritiogenic ^{3}Helium component from the atmospheric component ($\alpha R_a \times {}^4He_s$), under the assumption that there are no other sources of dissolved helium.

We applied both approaches (Equations 3 and 4) to estimate the downward advective velocity of porewater through the peat profile. Because tritium concentrations in precipitation vary both intra- and inter-annually due to atmospheric processes and anthropogenic emissions, we compared the vertical tritium concentration profile to the variation of tritium in precipitation recorded at the Ottawa station of the Global Network of Isotopes in Precipitation (GNIP/IAEA, 2021). Ottawa precipitation levels were decay-corrected and scaled to the tritium level in local precipitation in 2015. This comparison was performed to confirm that higher levels of tritium at greater depths coincided with elevated levels of tritium in historical precipitation.

We used the resulting advection estimate to calculate DIC production rates by fitting the advection-diffusion equation to each DIC depth profile (Figure S2 in Supporting Information S1).

$$\frac{\partial C}{\partial t} = Ds\,\varphi \frac{\partial^2 C}{\partial x^2} - v\,\varphi \frac{\partial C}{\partial x} + R \tag{6}$$

Where C is the DIC concentration, D_s is the diffusion coefficient for CO_2 in water corrected for temperature, φ is the porosity of the peat at each depth, v is the previously calculated advection rate, x is the depth, t is time, and R is the rate of production. Assuming steady-state or $\frac{\partial C}{\partial t} = 0$, we were then able to solve for R, the production rate of DIC. The derivatives of DIC concentration with respect to depth were calculated from the depth profiles which were well fit by a logarithmic equation (Figure S2 in Supporting Information S1). The production rate is then just the difference between the diffusion and advection terms. Since the concentration of DIC in all depths was less than the theoretical solubility limit (12 mM), we assumed that gaseous CO_2 loss was negligible. We then multiplied rates by 2 to account for both CO_2 and CH_4 production which we assume occur in a 1:1 ratio (as per Conrad, 1999). This theoretical ratio, likely overestimates decomposition at most depths, especially in the surface as peatlands are widely known to deviate from the theoretical 1:1 CO_2:CH_4 production ratio (Nilsson & Öquist, 2009; Wilson et al., 2017). Empirical measurements of CO_2:CH_4 ratios in the porewater at the site show that below 25 cm, the CO_2:CH_4 declines with warming from about 2:1 in the ambient enclosure to just over 1:1 at the warmest treatments (Wilson et al., 2021). Once total production rates were calculated, using Equation 6, multiplication by the fraction of peat contribution to total production, calculated from Equation 1, yields the estimated peat loss. To then compare our estimated rates with Hanson et al. (2020) we fit peat losses to exponential curves as a function of peat depth and integrated those profiles (from the surface to 3 m) to get the rates in g C m^{-2} y^{-1}.

3. Results

3.1. Radiocarbon and DOC Results

The radiocarbon of the dissolved inorganic carbon ($DI^{14}C$) appears more depleted in the +6.75 °C and +9 °C treatments both over time within each enclosure and relative to the ambient enclosure and control plots (Figure 1). While the $DI^{14}C$ is similar to the control and ambient enclosures prior to the initiation of heating treatments, the isotopic depletion evolves over the course of the study (Figure 1) approaching up to 50‰ depletion relative to the ambient enclosure at 2 m deep. It has been shown empirically that the $DI^{14}C$ is representative of the CH_4 produced in the system (Chanton et al., 2008; Clymo & Bryant, 2008; Wilson et al., 2016). The similarity of $\Delta^{14}C$ of CO_2 and CH_4 makes theoretical sense as well because CH_4 is either

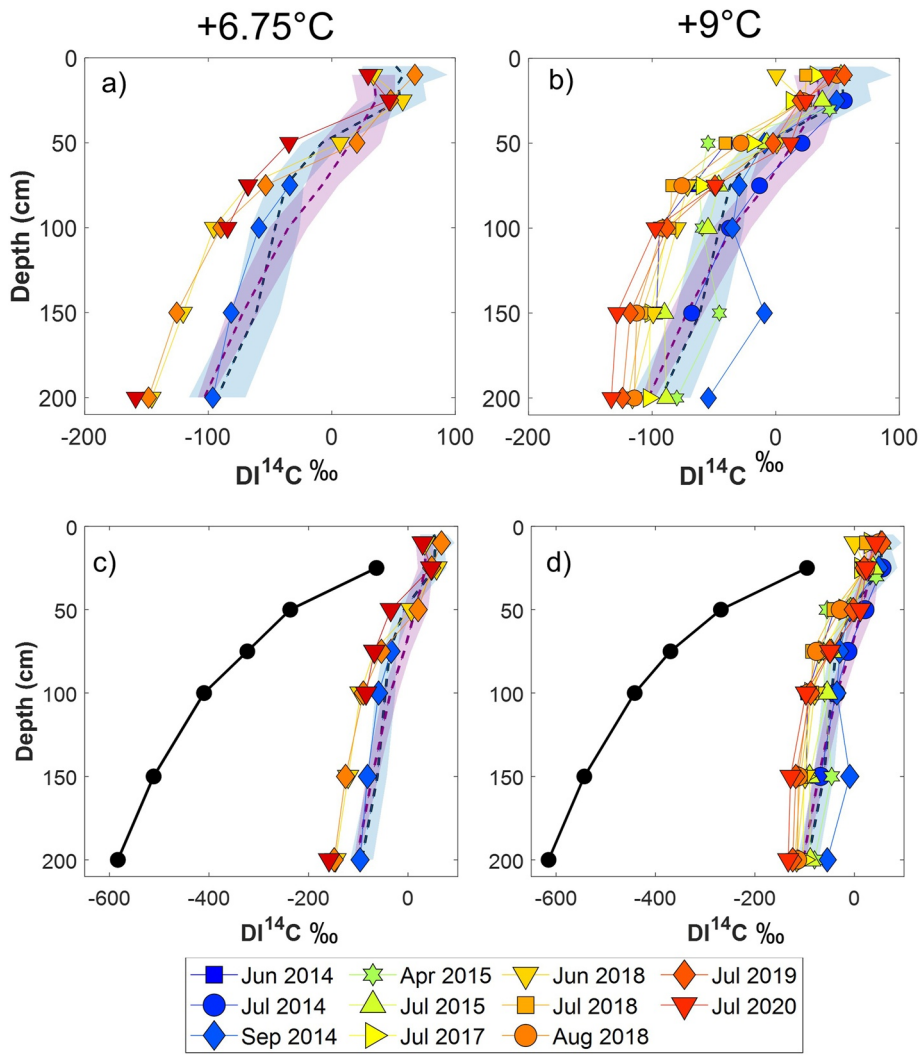

Figure 1. Radiocarbon content of the porewater dissolved inorganic carbon in the +6.75 °C (panel a) and the +9 °C (panel b) treatments, with sampling dates represented by symbols. Panels c and d present the same dissolved constituent data on expanded axes and include the solid peat ^{14}C profiles (black circles) for the +6.75 °C and +9 °C plots respectively. The solid peat was measured only in 2012, prior to the warming treatment, as the ^{14}C of the solid peat is not expected to change rapidly. Dashed lines indicate the locally weighted polynomial regression curves of the ambient enclosure and control plots (plot 6 = pink and plot T3F = blue, respectively) from 2014-2020 with the ±95% confidence interval indicated by the shaded area around each line (MATLAB, 2020). Due to budgetary constraints, radiocarbon in the +6.75 °C treatment was not routinely measured until 2018.

produced from the reduction of CO_2 with H_2, or from acetate dissimilation which produces both CO_2 and CH_4, and because $\Delta^{14}C$ is corrected for mass-dependent fractionation.

Because dissolved porewater cations of calcium and magnesium are low in the upper 3 m of the peat column at SPRUCE relative to the surrounding groundwater aquifer (Griffiths & Sebestyen, 2016; Griffiths et al., 2019), groundwater is thought to have little influence on DIC. Porewater pH averages from about 4 at the surface to around 5.5 at 2 m deep (Sebestyen & Griffiths, 2016). Thus, porewater DIC at this site results from microbial respiration of available organic C which could be either from the peat or DOC. The radiocarbon depletion of the DOC at a particular depth could be strongly influenced by the downward advection of surface-produced DOC or could result from leaching of the labile or soluble forms of C of the peat at a given depth. To explore which of these effects was dominating, we focus here on the DO^{14} C with depth in the ambient, +6.75° and +9 °C treatment enclosures (Figure 2). The radiocarbon values of the DOC in the

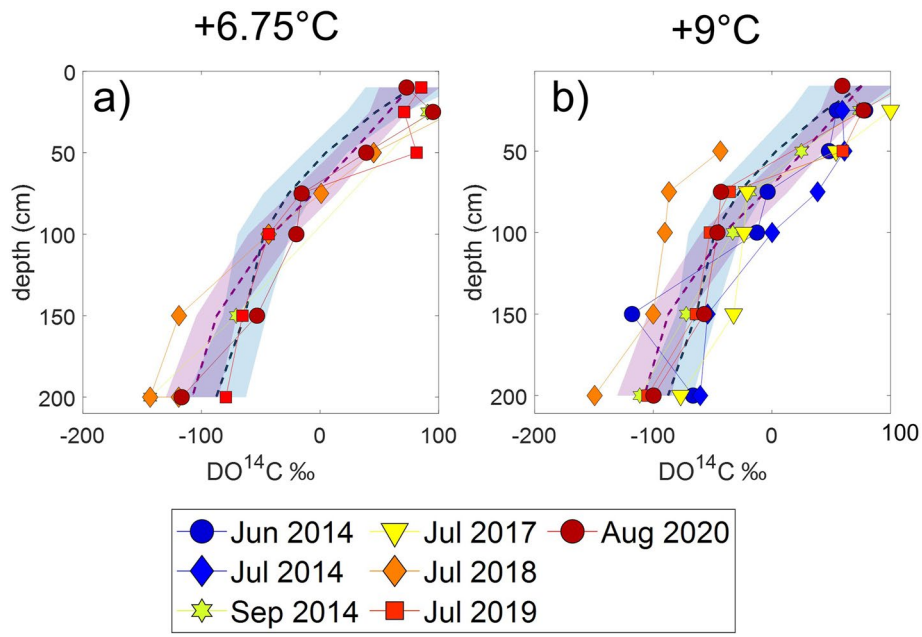

Figure 2. Radiocarbon content of the porewater dissolved organic carbon in the +6.75 °C (panel a) and the +9 °C (panel b) treatments, with sampling dates represented by symbols. Dashed lines indicate the locally weighted polynomial regression of the ambient enclosure and control plots (plot 6 = pink and plot T3F = blue, respectively) from 2014-2020 with the ±95% confidence interval indicated by the shaded area around each line (MATLAB, 2020). Due to budgetary constraints, radiocarbon in the +6.75 °C treatment was not routinely measured until 2018.

+6.75 °C and +9 °C enclosures were, in nearly every case, either more positive than the DOC in the unheated plots or within the 95% confidence intervals over the experiment through July 2020 (Figure 2).

Unlike the DIC results, the heated plots do not appear to produce DOC that is markedly different than that found in the unheated plots. When the radiocarbon content of the DIC was compared to DOC for the same plot, the 95% confidence intervals calculated over all years of the $DI^{14}C$ overlapped those of the $DO^{14}C$ in the unheated plots (Figures 3a and 3b), but in the heated treatments, the $DI^{14}C$ appeared depleted relative to the $DO^{14}C$ (Figures 3c and 3d).

DOC concentrations increased with temperature in the top 25 cm (Figure 4). In the surface (<25 cm), the mean DOC concentrations were lowest in the ambient treatment and concentration generally increased with temperature treatment (Figure 4). Below a subsurface maximum typically around 75 cm, DOC concentrations declined with depth in all plots and the differences in concentrations among the different treatments became smaller (Figure 4). The overall decline in the DOC concentration in the heated enclosures from the surface to 1 m was roughly 7.5 mM. DIC concentrations also increased with temperature treatment in the top 25 cm. In contrast to the DOC profiles, DIC concentrations increased with depth in all temperature treatments including the ambient enclosure. DIC concentrations at a depth of 200 cm were similar (5 mM) for all temperature treatments. Mineralization to DIC dominated CH_4 production (Hopple et al., 2020), thus, DOC was consumed with depth faster than could be accounted for by CO_2 and CH_4 production alone, so that there must be another source for DOC loss.

Lateral advection, particularly along shallow subsurface flow paths in peatlands (Griffiths et al., 2019; Urban et al., 1989, 2011), greatly contributes to DOC losses from peatlands to outlet streams (Sebestyen, Lany, et al., 2021). However, in our analysis there was no significant correlation between DIC and DOC concentration in the outflows draining the enclosures (Figure S3 in Supporting Information S1), and other studies have shown the lateral flow of C is minimal at this site (Hanson et al., 2020). Further, lateral losses of DOC should not cause a discrepancy between DOC loss and DIC and CH_4 production rates in porewater since the lateral advection of water should carry both proportionally. Thus, lateral losses are not expected to influence the relationship in porewater.

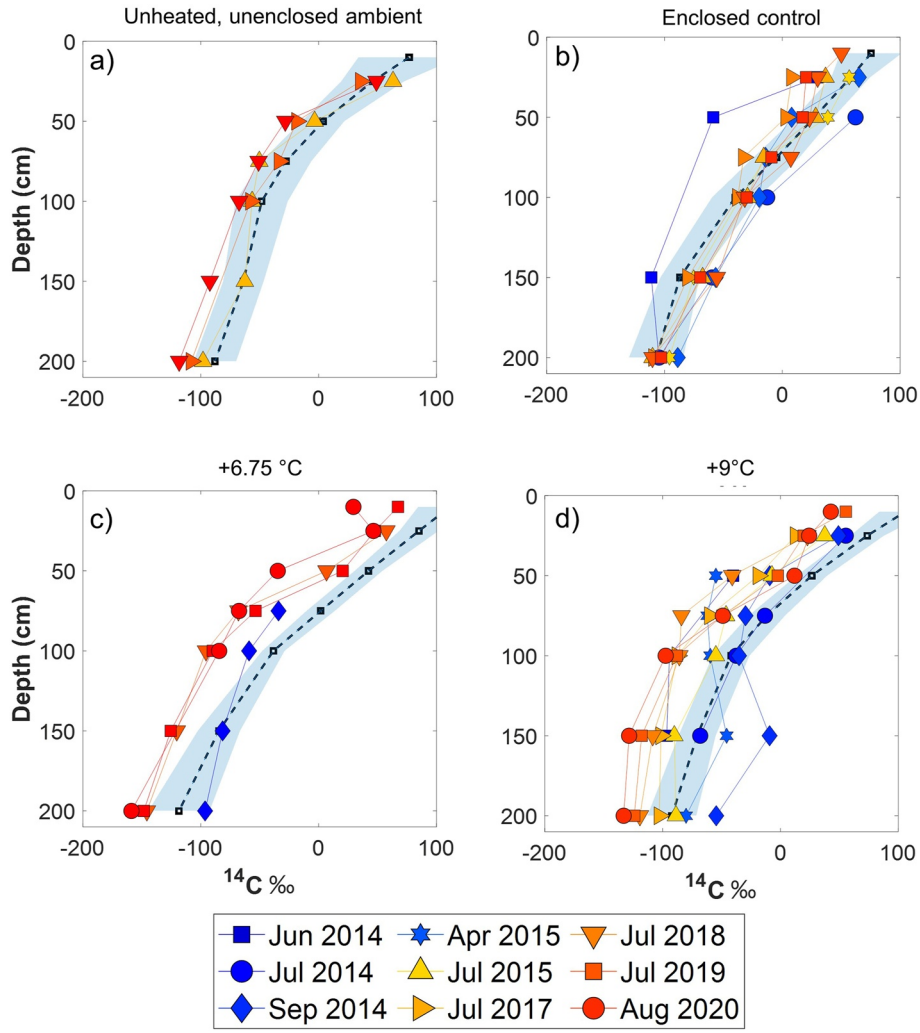

Figure 3. Comparing radiocarbon of respiration product, dissolved inorganic carbon with presumed substrate dissolved organic carbon. Dashed lines are the locally weighted polynomial regression for the DO^{14} C over all years 2014–2020 ± 95% confidence intervals indicated by the shaded blue line (MATLAB, 2020). Profiles of DI^{14} C by date are represented by symbols connected by lines, colors for each profile grade from blue (2014) to dark red (2020) over the time of the experiment. Panel (a) gives the results for the unheated, unenclosed ambient (T3F) plot. Panel (b) provides the enclosed control, panel (c) provides the +6.75 °C treatment enclosure, and panel (d) gives the +9 °C treatment enclosure.

In the outflows from each enclosure, there was a significant positive correlation between DI^{13} C and the concentrations of DIC (Figure 5a) and a significant negative correlation between the DI^{13} C and the concentration of DOC (Figure 5b). Stable isotopic fractionation occurs during microbial C processing due largely to kinetic isotope effects (Whiticar, 1999). In general, the lighter isotope reacts faster by an amount that is roughly proportional to the mass difference between the compound containing the abundant isotope and the compound containing the heavier isotope. Since the DOC concentration was always >2.5 mM (Figure 4), substrate limitation was unlikely. During microbial reduction of CO_2 to CH_4, the light isotope is preferred such that the remaining CO_2 pool becomes enriched as methanogenesis progresses. As total heterotrophic respiration increased with temperature, overall, there was also a significant correlation between δ^{13}C of the DIC and DIC concentrations in the outflows from each enclosure (Figure 5a) consistent with other reports that decomposition is also becoming increasingly methanogenic as warming is applied to enclosures at SPRUCE (e.g., Hopple et al., 2020; Wilson et al., 2016). These findings suggest that when DOC is abundant, decomposition is shifted toward CO_2 production, but as decomposition progresses and fresh DOC is depleted, resulting in a lower normalized C oxidation state (Wilson et al., 2021), the system shifts

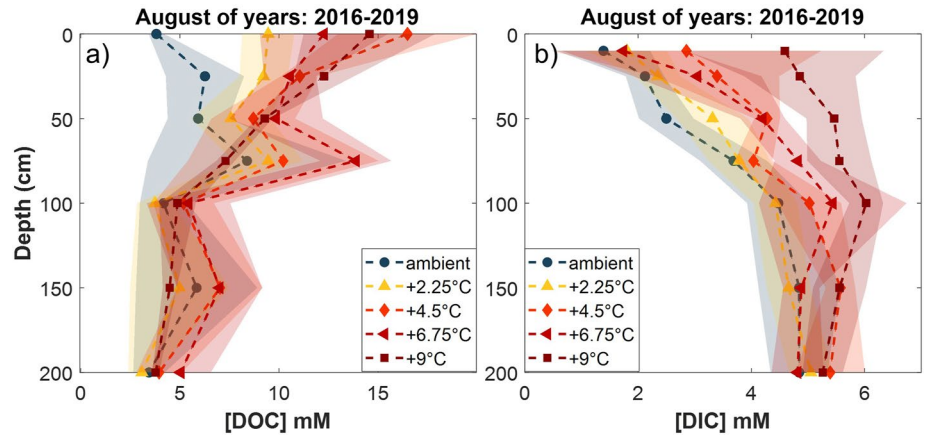

Figure 4. Depth profiles of DOC concentrations (panel a) and DIC concentrations (panel b) with depth in the peat measured in August every year from 2016-2019 in all treatment enclosures (+0 to +9 °C, ambient CO_2 only). Dashed lines indicate the DOC locally weighted polynomial regression (LOESS) and shaded region indicates the ±95% confidence interval for each enclosure over the time range 2016–2019. Colors grade from dark blue in the ambient (Plot 6) to dark red in the warmest treatment plots.

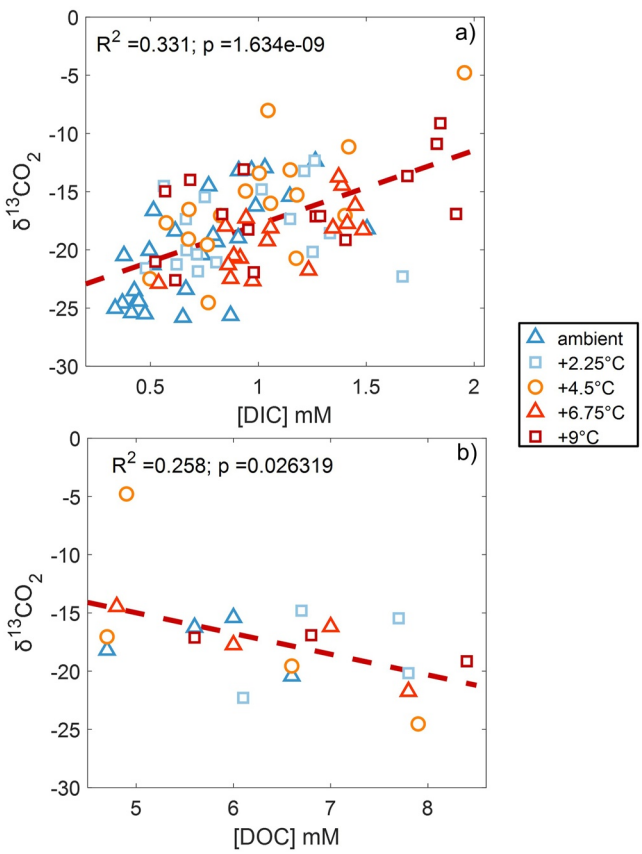

Figure 5. Correlations of the ^{13}C content of the DIC ($\delta^{13}CO_2$) with DIC concentration on all dates in 2016 and 2017 (panel a) and total dissolved organic carbon concentrations in August 2016 (panel b) in the enclosure outflows which drain the 50 cm depth. Dashed red lines indicate regression results with regression parameters listed in the top left of each panel.

increasingly toward methanogenesis. This is consistent with the findings of Rush et al. (2021) that terminal electron acceptor availability was not correlated with temperature, but rather that faster reduction of the organic matter pool in the surface leads to increasing methanogenesis.

3.2. Modeling

In many, though not all, enclosures and dates, the calculated contribution of peat to DIC production increased to 75–100 cm and then leveled off (Figure 6). Below that depth, the contribution of peat to total respiration was generally stable with depth up to 2 m. In the heated enclosures (Figures 6b and 6c), there was a trend of increasing contribution of peat to total DIC production relative to the dates before heating differentials were reached (blue symbols).

The average ^3H concentration measured in 10 precipitation samples collected at the site was 28.2 ± 5.9 (±1 s.d.) pCi L^{-1}. The values range from 18.8 pCi L^{-1} to 39.0 pCi L^{-1}. The measurement uncertainty of the reported data ranges from 0.8 pCi L^{-1} to 2.5 pCi L^{-1}. The average porewater ^3H concentration at 0 cm was 28.4 ± 0.7 pCi L^{-1} (Figure S4 in Supporting Information S1), that is, not significantly different from the precipitation value. The average ^3H concentrations decreased down the porewater profile to 24.9 ± 2.2 pCi L^{-1} at 2 m depth (Figure S4 in Supporting Information S1). We found similar patterns of decreasing concentrations with depth across all plots and both dates. Assuming steady-state inputs of tritium at the surface, the decrease in ^3H activity corresponds to tritium ages up to 2.2 ± 1.3 years at 100 cm which translates to a downward advective velocity of 45 cm. This is a reasonable value given the annual precipitation of ~800 mm and a peat porosity approaching 1 at the surface (Verry, Boelter, et al., 2011). Below 100 cm, porewater ^3H increased at the 200 cm depth (29.4 ± 3.1 pCi L^{-1}). We will show this is caused by historical variation of precipitation ^3H.

There was no accumulation of tritiogenic ^{3}Helium in the top 100 cm of the porewater profile (Figure S4 in Supporting Information S1). We

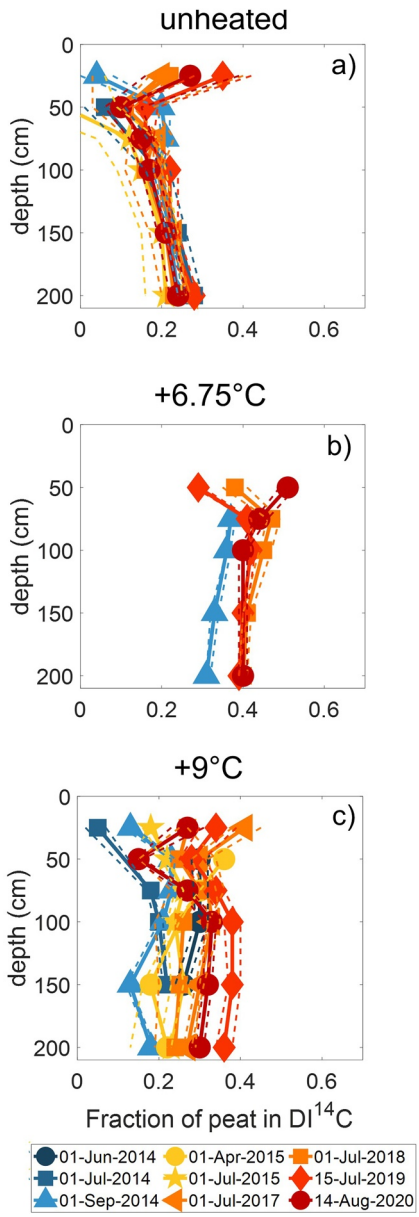

Figure 6. Results of the mass balance calculating the fraction of peat contribution to the total DIC for panel (a) = ambient enclosure, panel (b) = +6.75 °C enclosure and panel (c) = +9 °C enclosures. Symbols represent the mean of each sampling date and dashed lines indicate the minimum and maximum of results using either the date-specific or date-averaged (over all dates) surface DOC radiocarbon values as the end-member.

attribute this to several pathways of exchange with the atmosphere, either via diffusion, ebullition, or plant-mediated gas exchange. Below 100 cm tritiogenic ^{3}Helium increased to the equivalent of 2.1 ± 2.6 pCi L^{-1} at 150 cm and 9.2 ± 4.3 pCi L^{-1} at 200 cm (Figure S4 in Supporting Information S1). This accumulation of tritiogenic ^{3}Helium, combined with tritium concentrations of 27.1 pCi L^{-1} at 150 cm depth (average of 100 and 200 cm) and 29.4 pCi L^{-1} at 200 cm results in ^{3}H/^{3}He ages of 1.4 ± 1.9 and 4.8 ± 1.8 years, corresponding to a vertical flow velocity of 21 cm y^{-1}. We combine these two age estimates by adding the tritium age of 2.2 years (at 100 cm depth) to the ^{3}H/^{3}He ages for greater depths (Figure S5 in Supporting Information S1). The resulting age profile corresponds to an average downward velocity of 32 ± 3 cm y^{-1} based on a linear regression through the origin (Figure S5 in Supporting Information S1).

As an independent check on our derived advection rates, historical concentrations of tritium in precipitation, recorded at the Ottawa GNIP station, were decay-corrected to the sample date (2015) and scaled to match the concentration of tritium in local precipitation in 2015. The monthly GNIP time-series was transposed to a vertical profile using the 32 cm yr^{-1} downward advective transport velocity (Figure S4 in Supporting Information S1). Decreasing concentrations of tritium in the top 100 cm match the values in historical precipitation between 2012 and 2015. The higher tritium concentration observed at 200 cm depth corresponds to elevated tritium levels in precipitation in 2009. The consistency with historical precipitation provides confidence that the pore water ages derived from tritium decay and tritium-^{3}Helium ratios validate our estimate of a downward flow velocity of 32 cm y^{-1}.

Integrated peat C loss rate calculations in the ambient enclosure were 15.0 ± 3.0 g C m^{-2} y^{-1}, in the +6.75 °C treatment were 18.2 ± 6.1 g C m^{-2} y^{-1}, and in the +9 °C treatment were 18.5 ± 5.7 g C m^{-2} y^{-1} (averaged over the years 2015–2020). These rates were slightly less but on the same order of CH_4 production rates calculated by Ma et al. (under review, 25–75 g C m^{-2} y^{-1}). However, they are an order of magnitude lower than the total C loss as CO_2 and CH_4 are estimated for the warmest enclosures by Hanson et al. (2020) using the SET method. The difference between our rates and those of Hanson et al. (2020) could be accounted for by ebullition and or plant transport-mediated C losses. In our advection-diffusion based estimates of DIC production, we assumed ebullition to be negligible based on solution concentrations less than saturation. However, we know that this assumption is not correct and that it is possible to form bubbles at concentrations less than saturation (e.g., Chanton et al., 1989). We estimated the amount of ebullition that would have needed to occur to account for the "missing" ~280 g C m^{-2} y^{-1} estimated by Hanson et al. (2020). To do this we assumed a bubble composition of $CO_2 + CH_4 = 33\%$ and $N_2 = 67\%$ based on values in Chanton et al. (1989). Although Chanton et al. (1989) were working in a freshwater marsh and not a peatland, we will show that this is a reasonable first approximation. Applying the ideal gas law and the assumed bubble composition, we estimate that a bubble flux of approximately 2 L m^{-2} d^{-1} could account for the ~280 g C m^{-2} y^{-1} difference between our estimates and those of Hanson et al. (2020). Plant gas transport would of course reduce the ebullitive flux estimate.

4. Discussion

The radiocarbon content of porewater DIC, one of the main microbial respiration products, has become increasingly ^{14}C depleted in the warmer treatment enclosures throughout the SPRUCE experiment (Figure 1). This finding, in itself clearly indicates that warming stimulates microorganisms to respire ^{14}C-depleted, ancient peat C that accumulated under prior climate conditions (i.e., cooler than the actively warmed treatments) that were more favorable to sequestration. In contrast, the radiocarbon content of DOC, the other probable substrate for microbial respiration, was generally positive in the top 50 cm (Figure 2) consistent with C fixed within the last century and in contrast with the much older peat (Figures 1c and 1d). DO^{14} C was not significantly more negative following warming compared to the same areas before heating began (Figure 2). This lends further support to the hypothesis that increasing mineralization of peat C, rather than DOC, is responsible for the altered isotopic signature of the DIC, although warming-induced losses of more positive ^{14}C fixed immediately following nuclear testing when atmospheric radiocarbon values were more positive could be masking the trends in DOC. Although, bomb carbon is useful as a tracer in itself (e.g., Dioumaeva et al., 2002), the low resolution sampling in the surface peat precluded us from using this approach (McFarlane et al., 2018). Nevertheless, the apparent destabilization of the large peat C reservoir has serious implications for peatland-climate feedbacks especially if the delicate balance of the peatland is tipped from a net C sink to a net C source (Griffiths et al., 2017; Hanson et al., 2020).

DOC concentrations in the surface (0–50 cm) porewater are significantly higher in the warmer enclosures compared to the unheated enclosure (Figure 4). This increase in DOC concentration with warming is likely a combined result of the accumulation of less bioavailable DOC, as well as shifts in the plant community increasingly toward rooted vascular plants in the warmest enclosures, increasing plant primary production (McPartland et al., 2020; Norby et al., 2019) with a concomitant increase in root exudation and litter deposition. While increasing plant productivity has the potential to partially offset C losses, it is likely that much of this C is also available to stimulate microbial respiration particularly on the surface where we observe increasing concentrations (Figure 4) and production (Hopple et al., 2020) of both CO_2 and CH_4. This increase in CH_4 production is striking because the higher greenhouse gas potential of CH_4 relative to CO_2 (IPCC, 2013; Neubauer & Megonigal,, 2015) means that increasing methanogenesis in the surface is likely to exacerbate peatland-climate feedbacks.

To further investigate the potential destabilization of peat C with warming, we calculated the relative amounts of DOC and peat needed to produce DIC with the observed radiocarbon values. DOC is thought to be the primary source of microbially produced DIC in peatlands (Hopple et al., 2020; Tfaily et al., 2014; Wilson et al., 2016) but peat represents the other plausible substrate. The radiocarbon of the DIC represented as $\Delta^{14}C$ is corrected for biological mass dependent fractionation using the $\delta^{13}C$, thus the DI^{14} C should reflect the mixing between the radiocarbon values of the two substrates. For all enclosures and depths studied, the contribution of peat to DIC was calculated to be less than 50% (Figure 6), consistent with the earlier reports that DOC is the primary substrate (Wilson et al., 2016) as well as observations from other peatlands (Chasar et al., 2000; Chanton et al., 2008). The subsurface maximum in peat contribution observed in many of the plots is consistent with observations made by Tfaily et al. (2018) regarding a subsurface zone of high microbial C cycling 50–100 cm below the peat surface. Additionally, it should be noted that immediately following the initiation of warming (2015) the contribution of peat to total DIC production was small and increased with prolonged warming (Figure 6c). However, there was a clear increase in the contribution of peat to DIC radiocarbon in the warmer treatments. This C from peat is consistent with the initial results post-initiation of deep peat heating suggesting that the peat C bank was stable (Wilson et al., 2016), but there is an apparent lag with the effects from warming leading to increased peat decomposition becoming more pronounced over time (Hopple et al., 2020). This lag could signify a kinetic limitation on peat decomposition under these conditions. Alternatively, increasing DOC in the surface of the warmer plots has been suggested to facilitate decomposition of the peat (e.g., Garnett et al., 2020) under the anaerobic and typically terminal electron acceptor (TEA)-depleted conditions (Rush et al., 2021; Wilson, Tfaily, et al., 2017) by increasing the availability of small metabolites necessary for growing microorganisms or the terminal electron acceptors needed to couple peat C oxidation. In other warming experiments, reduced C accumulation with warming has been attributed to an increased thickness of the acrotelm, that is, larger aerobic layer (e.g., Bridgham et al., 2008; Chen et al., 2008; Samson et al., 2018), Here, we show that after a short lag period anaerobic

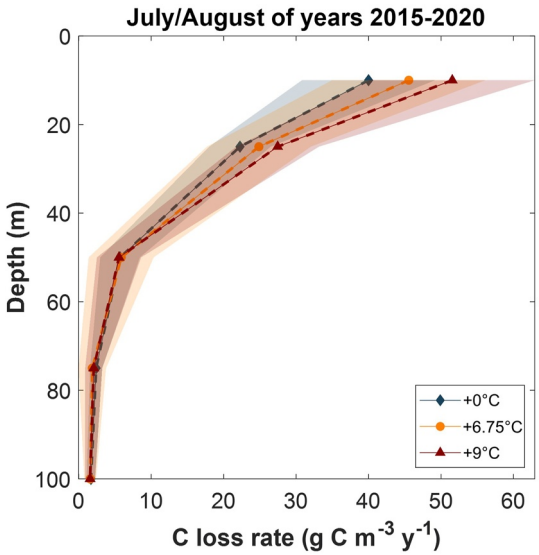

Figure 7. Peat carbon loss versus depth profile for the unheated (Plot 6), +6.75 °C (Plot 8), and +9 °C (Plot 17) treatments dashed lines indicate the locally weighted polynomial regression (LOESS) and shaded region the ±95% CI over July and August from 2015-2020. Points indicate average estimates for each depth with shading outlining the 95% confidence interval.

peat decomposition also increases with temperature treatment leading to loss of previously deposited C.

If a non-diffusive transport (e.g., ebullition, plant transport) rate of 2 L m^{-2} d^{-1} is assumed, our C loss calculations reasonably match the C balance of Hanson et al. (2020). A bubbling rate of 2 L m^{-2} d^{-1} is within the range of rates measured at other sites (e.g., Stamp et al., 2013). However, our calculation assumes steady bubbling throughout the winter, when it is likely that ebullition is lower due to snow and ice cover acting as a confining layer to bubble transport as well as overall lower production rates in colder temperatures. Although temperatures in the deep peat (2 m) only vary by about 4 °C over the course of a year (Hanson et al., 2017; Wilson et al., 2016), most of the CO_2 and CH_4 production occurs above 50 cm (Figure 7) where temperatures in the winter can be as low as 6 °C and in the summer as high as 17 °C, a range which is associated with a large change in both CO_2 and CH_4 production potential (Kolton et al., 2019). Nevertheless, bubbles could build up throughout the winter months and then "burp" during melt leading to high variability in bubble rates over time which is not well-represented in the SPRUCE monitoring efforts. Ma et al. (2017) estimated ebullition and plant transport rates at SPRUCE of up to 200 g C m^{-2} y^{-1}, with plant-mediated transport making up ~85% of that rate. Considering plant transport, the average 2 L m^{-2} d^{-1} of net non-diffusive transport needed to reconcile our calculations with measurements made in Hanson et al. (2020) is not unreasonable.

Bulk peat as it is used here to calculate the fraction contribution of peat to DIC production, is actually a complex mixture of aged peat, dead roots, newly dead plant material, and live roots, especially near the surface. DOC can be released from or decomposed differentially in each of these forms. Presumably, the newly dead plant material portion of the bulk peat would be more labile than the fraction of peat remaining in a horizon increment that has been present over many years. Below the active rooting depth (40 cm; Iversen et al., 2018), the mixture becomes much simpler and is likely to represent primarily aged peat. The variability in the fractional peat contributions to total microbial DIC production in the top 40 cm (Figure 6) is consistent with the complex nature of the bulk peat in the surface depth where live plants and freshly deposited organic matter are contributing. Nevertheless, below 40 cm where aged peat likely dominates the bulk peat, is where there is the strongest evidence for increasing contribution of peat C to total DIC production with warming. Additional analyses will be needed to fully resolve the various fractions and their contributions in the surface peat, but for now, it seems clear that below the depth where live and freshly dead plants influence, there is increasing aged peat C losses as the system warms.

The warming treatment at SPRUCE includes temperatures up to +9 °C above ambient (Hanson et al., 2011, 2017). While greater than many end-of-century climate warming projections for the latitude of the SPRUCE experiment, +9 °C is within the upper trajectory of highest predictions possible by 2100 for northern latitudes (Schädel et al., 2016) which will experience the greatest climatic warming effects (Collins et al., 2013). In addition, there could be transient temperature excursions that exceed mean predictions and, given current greenhouse gas production rates, warming greater than predicted is increasingly likely (Christensen et al., 2007). Finally, exploring the response to warming across a range of treatment levels including, this high end of local warming predictions, allows non-linear curve fitting crucial to detecting threshold ecosystem responses (Amthor et al., 2010) or tipping points (e.g., Eppinga et al., 2009).

The differences in porewater DOC concentrations among the treatments narrow with increasing depth in the peat (Figure 4). This concentration convergence at depth occurs despite that the temperature differential among the plots increases with depth due to energy losses at the surface (e.g., Wilson et al., 2016) since we would expect leaching to be greater at warmer temperatures (Whitworth et al., 2014). This is evidence that the increase in DOC concentration is not simply from the leaching of the peat. While we infer vertical advection of water at the site to be on the order of 30 cm y^{-1}, such vertical advection would not account

for the unexpectedly strong decline in DOC concentrations, relative to the increase in microbial respiration products, since the DOC concentration is higher at the surface and advection would have the effect of contributing DOC to depth rather than diluting the DOC that was already there. In another study, lateral advection resulted in C losses, but only accounted for about 2 mM y^{-1} of combined DIC and DOC (Hanson et al., 2020) and would not explain the sharp decline observed with depth in our profiles.

The curve fitting approach used in the modeling here is strongly influenced by the downward advection rate, which we calculated from the ^{3}H to be 32 cm y^{-1}. This rate was averaged over three of the treatment enclosures and two sampling dates (Plots 6, 13, and 17). It is highly likely that advection rates vary considerably both spatially and temporally. For example, it is hypothesized that advection rates are highest immediately the following snowmelt when large amounts of water are being input to the system with a pulse of snowmelt-derived water in a few short weeks. Advection rates are possibly considerably slower in the late summer when the system is drier. Alternatively, advection could be enhanced following large rain events in a series of repeated pulses throughout the year. Higher spatial and temporal resolution sampling across the site could prove useful for further constraining advection rates in this system.

Peatlands historically act as important C sinks. Carbon accumulation in peatlands was generally high during early establishment, followed by a millennia-long decline in accumulation rates and then an increase in accumulation rates during the last 100 years before present (Garneu et al., 2014; Loisel et al., 2014; McFarlane et al., 2018; Van Bellen, Dallaire, et al., 2011; Van Bellen, Garneau, et al., 2011). The mean C accumulation rate at the S1 bog in the early Holocene was 30 ± 6 g C m^{-1} y^{-1}, which declined to 15 ± 8 g C m^{-2} y^{-1} in the late Holocene, but increased to 74 ± 57 g C m^{-2} y^{-1} in the last century based on detailed ^{14}C analyses (Iversen et al., 2012; McFarlane et al., 2018). Our estimate of C losses on the order of 20 g C m^{-2} y^{-1} offsets a large percentage of that sink potential with strong implications for peatland-climate feedbacks. Our results suggest that these peatland-climate feedbacks are exacerbated with continued warming. Previous results from 13 months following initiation of deep peat heating at the SPRUCE site did not provide evidence of significant contributions of peat C to microbial respiration and concluded that the peat C bank was stable to warming temperatures (Wilson et al., 2016). However, results in this study and others (e.g., Hanson et al., 2020; Hopple et al., 2020) have demonstrated that those previous measurements were collected during an apparent lag period and there is now a growing body of evidence (Hanson et al., 2020; Hopple et al., 2020; Wilson et al., 2021) that the peat in the S1 bog is being destabilized by the warming treatment.

Acknowledgments
This study was funded in part by the Office of Biological and Environmental Research, Terrestrial Ecosystem Science Program, under United States DOE contracts DE-SC0007144 and DE-SC0012088. Oak Ridge National Laboratory is managed by UT-Battelle, LLC, for the U.S. Department of Energy under contract DE-AC05-00OR22725. Work performed at LLNL under Contract DE-AC52-07NA27344 with funding from Laboratory Directed Research and Development (14-ERD-038). The participation of Randall K. Kolka and Stephen D. Sebestyen was funded by the Northern Research Station of the USDA Forest Service. Measurement of DOC concentration at the Forestry Sciences Laboratory, Grand Rapids, MN, was also funded by the USDA Forest Service. This manuscript has been co-authored by UT-Battelle, LLC under Contract No. DE-AC05-00OR22725 with the U.S. Department of Energy. The United States Government retains and the publisher, by accepting the article for publication, acknowledges that the United States Government retains a non-exclusive, paid-up, irrevocable, worldwide license to publish or reproduce the published form of this manuscript, or allow others to do so, for United States Government purposes. The Department of Energy will provide public access to these results of federally sponsored research in accordance with the DOE Public Access Plan (http://energy.gov/downloads/doe-public-access-plan).

Data Availability Statement

All data presented in this manuscript and the Supplemental Appendix files, including figure source data, are publicly available from the SPRUCE long-term repository (https://doi.org/10.25581/spruce.097/1825084). Tritium and noble gas data are available at https://doi.org/10.25581/spruce.069/1532523.

References

Amthor, J. S., Hanson, P. J., Norby, R. J., & Wullschleger, S. D. (2010). A comment on 'Appropriate experimental ecosystem warming methods by ecosystem, objective, and practicality' by Aronson and McNulty. *Agriculture Forest Meteorology*, *150*, 497–498. https://doi.org/10.1016/j.agrformet.2009.11.020

Bjorkman, A. D., Myers-Smith, I. H., Elmendorf, S. C., Normand, S., Rüger, N., Beck, et al. (2018). Plant functional trait change across a warming tundra biome. *Nature*, *562*(7725), 57–62.

Blagodatskaya, E., & Kuzyakov, Y. (2008). Mechanisms of real and apparent priming effects and their dependence on soil microbial biomass and community structure: Critical review. *Biology and Fertility of Soils*, *45*(2), 115–131. https://doi.org/10.1007/s00374-008-0334-y

Boumans, R. M., & Day, J. W. (1993). High precision measurements of sediment elevation in shallow coastal areas using a sedimentation-erosion table. *Estuaries*, *16*(2), 375–380. https://doi.org/10.2307/1352509

Bridgham, S. D., Pastor, J., Dewey, B., Weltzin, J. F., & Updegraff, K. (2008). Rapid carbon response of peatlands to climate change. *Ecology*, *89*(11), 3041–3048. https://doi.org/10.1890/08-0279.1

Burke, E. J., Chadburn, S. E., & Ekici, A. (2017). A vertical representation of soil carbon in the JULES land surface scheme (vn4. 3_permafrost) with a focus on permafrost regions. *Geoscientific Model Development*, *10*(2), 959–975. https://doi.org/10.5194/gmd-10-959-2017

Cahoon, D. R., Lynch, J. C., Perez, B. C., Segura, B., Holland, R. D., Stelly, C., et al. (2002). High-precision measurements of wetland sediment elevation: II. The rod surface elevation table. *Journal of Sedimentary Research*, *72*(5), 734–739. https://doi.org/10.1306/020702720734

Chanton, J. P., Glaser, P. H., Chasar, L. S., Burdige, D. J., Hines, M. E., Siegel, D. I., et al. (2008). Radiocarbon evidence for the importance of surface vegetation on fermentation and methanogenesis in contrasting types of boreal peatlands. *Global Biogeochemical Cycles*, *22*(4). https://doi.org/10.1029/2008gb003274

Chanton, J. P., Martens, C. S., & Kelley, C. A. (1989). Gas transport from methane-saturated, tidal freshwater and wetland sediments. *Limnology & Oceanography*, *34*(5), 807–819. https://doi.org/10.4319/lo.1989.34.5.0807

Chasar, L. S., Chanton, J. P., Glaser, P. H., & Siegel, D. I. (2000). Methane concentration and stable isotope distribution as evidence of rhizospheric processes: Comparison of a fen and bog in the Glacial Lake Agassiz Peatland complex. *Annals of Botany*, *86*(3), 655–663. https://doi.org/10.1006/anbo.2000.1172

Chen, J., Bridgham, S., Keller, J., Pastor, J., Noormets, A., & Weltzin, J. F. (2008). Temperature responses to infrared-loading and water table manipulations in peatland mesocosms. *Journal of Integrative Plant Biology*, *50*(11), 1484–1496. https://doi.org/10.1111/j.1744-7909.2008.00757.x

Christensen, T. R., Johansson, T., Olsrud, M., Ström, L., Lindroth, A., Mastepanov, M., et al. (2007). A catchment-scale carbon and greenhouse gas budget of a subarctic landscape. *Philosophical Transactions of the Royal Society A: Mathematical, Physical & Engineering Sciences*, *365*(1856), 1643–1656. https://doi.org/10.1098/rsta.2007.2035

Clymo, R. S., & Bryant, C. L. (2008). Diffusion and mass flow of dissolved carbon dioxide, methane, and dissolved organic carbon in a 7-m deep raised peat bog. *Geochimica et Cosmochimica Acta*, *72*(8), 2048–2066. https://doi.org/10.1016/j.gca.2008.01.032

Collins, M., Knutti, R., Arblaster, J., Dufresne, J. L., Fichefet, T., Friedlingstein, P., et al. (2013). Long-term climate change: Projections, commitments and irreversibility. In *Climate change 2013—The physical science basis: Contribution of working group I to the fifth assessment report of the intergovernmental panel on climate change* (pp. 1029–1136). Cambridge University Press.

Conrad, R. (1999). Contribution of hydrogen to methane production and control of hydrogen concentrations in methanogenic soils and sediments. *FEMS Microbiology Ecology*, *28*(3), 193–202. https://doi.org/10.1111/j.1574-6941.1999.tb00575.x

Dioumaeva, I., Trumbore, S., Schuur, E. A., Goulden, M. L., Litvak, M., & Hirsch, A. I. (2002). Decomposition of peat from upland boreal forest: Temperature dependence and sources of respired carbon. *Journal of Geophysical Research*, *107*(D3). https://doi.org/10.1029/2001jd000848

Elmendorf, S. C., Henry, G. H., Hollister, R. D., Björk, R. G., Bjorkman, A. D., Callaghan, T. V., et al. (2012). Global assessment of experimental climate warming on tundra vegetation: Heterogeneity over space and time. *Ecology Letters*, *15*(2), 164–175. https://doi.org/10.1111/j.1461-0248.2011.01716.x

Eppinga, M. B., De Ruiter, P. C., Wassen, M. J., & Rietkerk, M. (2009). Nutrients and hydrology indicate the driving mechanisms of peatland surface patterning. *The American Naturalist*, *173*(6), 803–818. https://doi.org/10.1086/598487

Euskirchen, E. S., Edgar, C. W., Turetsky, M. R., Waldrop, M. P., & Harden, J. W. (2014). Differential response of carbon fluxes to climate in three peatland ecosystems that vary in the presence and stability of permafrost. *Journal of Geophysical Research Biogeosciences*, *119*, 1576–1595. https://doi.org/10.1002/2014JG002683

Garneau, M., van Bellen, S., Magnan, G., Beaulieu-Audy, V., Lamarre, A., & Asnong, H. (2014). Holocene carbon dynamics of boreal and subarctic peatlands from Québec, Canada. *The Holocene*, *24*(9), 1043–1053. https://doi.org/10.1177/0959683614538076

Garnett, M. H., Hardie, S. M., & Murray, C. (2020). Radiocarbon analysis reveals that vegetation facilitates the release of old methane in a temperate raised bog. *Biogeochemistry*, *148*(1), 1–17. https://doi.org/10.1007/s10533-020-00638-x

Griffiths, N. A., Hanson, P. J., Ricciuto, D. M., Iversen, C. M., Jensen, A. M., Malhotra, A., et al. (2017). Temporal and spatial variation in peatland carbon cycling and implications for interpreting responses of an ecosystem-scale warming experiment. *Soil Science Society of America Journal*, *81*(6), 1668–1688. https://doi.org/10.2136/sssaj2016.12.0422

Griffiths, N. A., & Sebestyen, S. D. (2016). Dynamic vertical profiles of peat porewater chemistry in a northern peatland. *Wetlands*, *36*(6), 1119–1130. https://doi.org/10.1007/s13157-016-0829-5

Griffiths, N. A., Sebestyen, S. D., & Oleheiser, K. C. (2019). Variation in peatland porewater chemistry over time and space along a bog to fen gradient. *Science of the Total Environment*, *697*, 134152. https://doi.org/10.1016/j.scitotenv.2019.134152

Hanson, P. J., Childs, K. W., Wullschleger, S. D., Riggs, J. S., Thomas, W. K., Todd, D. E., & Warren, J. M. (2011). A method for experimental heating of intact soil profiles for application to climate change experiments. *Global Change Biology*, *17*(2), 1083–1096. https://doi.org/10.1111/j.1365-2486.2010.02221.x

Hanson, P. J., Griffiths, N. A., Iversen, C. M., Norby, R. J., Sebestyen, S. D., Phillips, J. R., et al. (2020). Rapid net carbon loss from a whole-ecosystem warmed Peatland. *AGU Advances*, *1*(3), e2020AV000163. https://doi.org/10.1029/2020av000163

Hanson, P. J., Riggs, J. S., Nettles, W. R., Phillipds, J. R., Krassovski, M. B., Hook, L. A., et al. (2017). Attaining whole-ecosystem warming using air and deep soil heating methods with an elevated CO_2 atmosphere. *Biogeosciences*, *14*, 861–883. https://doi.org/10.5194/bg-14-861-2017

Holden, J. (2005). Peatland hydrology and carbon release: Why small-scale process matters. *Philosophical Transactions of the Royal Society A: Mathematical, Physical & Engineering Sciences*, *363*(1837), 2891–2913. https://doi.org/10.1098/rsta.2005.1671

Hopple, A. M., Pfeifer-Meister, L., Zalman, C. A., Keller, J. K., Tfaily, M. M., Wilson, R. M., et al. (2019). Does dissolved organic matter or solid peat fuel anaerobic respiration in peatlands? *Geoderma*, *349*, 79–87. https://doi.org/10.1016/j.geoderma.2019.04.040

Hopple, A. M., Wilson, R. M., Kolton, M., Zalman, C. A., Chanton, J. P., Kostka, J., et al. (2020). Massive peatland carbon banks vulnerable to rising temperatures. *Nature Communications*, *11*(1), 1–7. https://doi.org/10.1038/s41467-020-16311-8

IAEA/WMO Global Network of Isotopes. (2021). *Precipitation*. The GNIP Database. Retrieved from https://nucleus.iaea.org/wiser

IPCC. (2013). Climate change 2013: The physical science basis. In T. F. Stocker, D. Qin, G.-K. Plattner, M. Tignor, S. K. Allen, J. Boschung, et al. (Eds.), *Contribution of working group I to the fifth assessment report of the intergovernmental panel on climate change* (p. 1535). Cambridge University Press. https://doi.org/10.1017/CBO9781107415324

Iversen, C. M., Childs, J., Norby, R. J., Ontl, T. A., Kolka, R. K., Brice, D. J., et al. (2018). Fine-root growth in a forested bog is seasonally dynamic, but shallowly distributed in nutrient-poor peat. *Plant and Soil*, *424*(1), 123–143. https://doi.org/10.1007/s11104-017-3231-z

Iversen, C. M., Murphy, M. T., Allen, M. F., Childs, J., Eissenstat, D. M., Lilleskov, E. A., et al. (2012). Advancing the use of minirhizotrons in wetlands. *Plant and Soil*, *352*(1), 23–39. https://doi.org/10.1007/s11104-011-0953-1

Keuper, F., Wild, B., Kummu, M., Beer, C., Blume-Werry, G., Fontaine, S., et al. (2020). Carbon loss from northern circumpolar permafrost soils amplified by rhizosphere priming. *Nature Geoscience*, *13*(8), 560–565. https://doi.org/10.1038/s41561-020-0607-0

Kolton, M., Marks, A., Wilson, R. M., Chanton, J. P., & Kostka, J. E. (2019). Impact of warming on greenhouse gas production and microbial diversity in anoxic peat from a Sphagnum-dominated bog (Grand Rapids, Minnesota, United States). *Frontiers in Microbiology*, *10*, 870. https://doi.org/10.3389/fmicb.2019.00870

Limpens, J., Berendse, F., Blodau, C., Canadell, J. G., Freeman, C., Holden, J., et al. (2008). Peatlands and the carbon cycle: From local processes to global implications—A synthesis. *Biogeosciences*, *5*(5), 1475–1491. https://doi.org/10.5194/bg-5-1475-2008

Loisel, J., Yu, Z., Beilman, D. W., Camill, P., Alm, J., Amesbury, M. J., et al. (2014). A database and synthesis of northern peatland soil properties and Holocene carbon and nitrogen accumulation. *The Holocene*, *24*(9), 1028–1042. https://doi.org/10.1177/0959683614538073

Ma, S., Jiang, J., Huang, Y., Shi, Z., Wilson, R. M., Ricciuto, D., et al. (2017). Data-constrained projections of methane fluxes in a northern Minnesota peatland in response to elevated CO_2 and warming. *Journal of Geophysical Research: Biogeosciences*, *122*(11), 2841–2861. https://doi.org/10.1002/2017jg003932

MATLAB. (2020). *MATLAB. Version 2020a*. The Math Works, Inc. Computer Software.

McFarlane, K. J., Hanson, P. J., Iversen, C. M., Phillips, J. R., & Brice, D. J. (2018). Local spatial heterogeneity of Holocene carbon accumulation throughout the peat profile of an ombrotrophic Northern Minnesota bog. *Radiocarbon*, *60*(3), 941–962. https://doi.org/10.1017/rdc.2018.37

McPartland, M. Y., Montgomery, R. A., Hanson, P. J., Phillips, J. R., Kolka, R. K., & Palik, B. (2020). Vascular plant species response to warming and elevated carbon dioxide in a boreal peatland. *Environmental Research Letters*, *15*, 124066. https://doi.org/10.1088/1748-9326/abc4fb

Merritt, D. A., Hayes, J. M., & Marais, D. J. D. (1995). Carbon isotopic analysis of atmospheric methane by isotope-ratio-monitoring gas chromatography-mass spectrometry. *Journal of Geophysical Research*, *100*(D1), 1317–1326. https://doi.org/10.1029/94jd02689

Neubauer, S. C., & Megonigal, J. P. (2015). Moving beyond global warming potentials to quantify the climatic role of ecosystems. *Ecosystems*, *18*(6), 1000–1013. https://doi.org/10.1007/s10021-015-9879-4

Nichols, D. S., & Peteet, D. M. (2019). Rapid expansion of northern peatlands and doubled estimated of carbon storage. *Nature Geoscience*, *12*, 917–921. https://doi.org/10.1038/s41561-019-0454-z

Nilsson, M., & Öquist, M. (2009). *Partitioning litter mass loss into carbon dioxide and methane in peatland ecosystems. Carbon cycling in northern peatlands* (pp. 131–144). American Geophysical Union.

Norby, R. J., Childs, J., Hanson, P. J., & Warren, J. M. (2019). Rapid loss of an ecosystem engineer: Sphagnum decline in an experimentally warmed bog. *Ecology and Evolution*, *9*(22), 12571–12585. https://doi.org/10.1002/ece3.5722

Ramaswamy, V., Boucher, O., Haigh, J., Hauglustaine, D., Haywood, J., Myhre, G., et al. (2001). Radiative forcing of climate change. In *Climate change 2001: The scientific basis—contribution of working group I to the third assessment report of the intergovernmental panel on climate change* (pp. 350–416). Cambridge University Press.

Romanov, V. V. (1961). *Hydrophysics of bogs (Gidrofizika bolot) (Israel Program for Scientific Translations)*. US Department of Agriculture.

Rush, J. E., Zalman, C. A., Woerndle, G., Hanna, E. L., Bridgham, S. D., & Keller, J. K. (2021). Warming promotes the use of organic matter as an electron acceptor in a peatland. *Geoderma*, *401*, 115303. https://doi.org/10.1016/j.geoderma.2021.115303

Samson, M., Słowińska, S., Słowiński, M., Lamentowicz, M., Barabach, J., Harenda, K., et al. (2018). The impact of experimental temperature and water level manipulation on carbon dioxide release in a poor fen in Northern Poland. *Wetlands*, *38*(3), 551–563. https://doi.org/10.1007/s13157-018-0999-4

Schädel, C., Bader, M. K. F., Schuur, E. A., Biasi, C., Bracho, R., Čapek, P., et al. (2016). Potential carbon emissions dominated by carbon dioxide from thawed permafrost soils. *Nature Climate Change*, *6*(10), 950–953. https://doi.org/10.1038/nclimate3054

Sebestyen, S. D., Funke, M. M., & Cotner, J. B. (2021). Sources and biodegradability of dissolved organic matter in two peatland catchments with different upland forest types, northern Minnesota, USA. *Hydrological Processes*, *35*(2), e14049. https://doi.org/10.1002/hyp.14049

Sebestyen, S. D., & Griffiths, N. A. (2016). *SPRUCE enclosure corral and sump system: Description, operation, and calibration. Carbon dioxide information analysis center*. Oak Ridge National Laboratory, US Department of Energy. https://doi.org/10.3334/CDIAC/spruce.030

Sebestyen, S. D., Griffiths, N. A., Oleheiser, K. C., & Stelling, J. M. (2020). *SPRUCE precipitation chemistry and bulk atmospheric deposition beginning in 2013*. Oak Ridge National Laboratory, Terrestrial Ecosystem Science Science Focus Area (TES SFA) & U.S. Department of Energy. https://doi.org/10.25581/spruce.085/1664397

Sebestyen, S. D., Griffiths, N. A., Oleheiser, K. C., Stelling, J. M., Pierce, C. E., Nater, E. A., et al. (2021). *SPRUCE outflow chemistry data for experimental plots beginning in 2016*. Oak Ridge National Laboratory, TES SFA, & U.S. Department of Energy. https://doi.org/10.25581/spruce.088/1775142

Sebestyen, S. D., Lany, N. K., Roman, D. T., Burdick, J. M., Kyllander, R. L., Verry, E. S., & Kolka, R. K. (2021). Hydrological and meteorological data from research catchments at the Marcell Experimental Forest, Minnesota, USA. *Hydrological Processes*, *35*, e14092. https://doi.org/10.1002/hyp.14092

Stamp, I., Baird, A. J., & Heppell, C. M. (2013). The importance of ebullition as a mechanism of methane (CH_4) loss to the atmosphere in a northern peatland. *Geophysical Research Letters*, *40*(10), 2087–2090. https://doi.org/10.1002/grl.50501

Surano, K., Hudson, G., Failor, R., Sims, J., Holland, R., MacLean, S., & Garrison, J. (1992). Helium-3 mass spectrometry for low-level tritium analysis of environmental samples. *Journal of Radioanalytical and Nuclear Chemistry*, *161*(2), 443–453. https://doi.org/10.1007/bf02040491

Tfaily, M. M., Cooper, W. T., Kostka, J. E., Chanton, P. R., Schadt, C. W., Hanson, P. J., et al. (2014). Organic matter transformation in the peat column at Marcell Experimental Forest: Humification and vertical stratification. *Journal of Geophysical Research: Biogeosciences*, *119*(4), 661–675. https://doi.org/10.1002/2013jg002492

Tfaily, M. M., Wilson, R. M., Cooper, W. T., Kostka, J. E., Hanson, P., & Chanton, J. P. (2018). Vertical stratification of peat pore water dissolved organic matter composition in a peat bog in northern Minnesota. *Journal of Geophysical Research: Biogeosciences*, *123*(2), 479–494. https://doi.org/10.1002/2017jg004007

Thomas, S., & Ridd, P. V. (2004). Review of methods to measure short time scale sediment accumulation. *Marine Geology*, *207*(1–4), 95–114. https://doi.org/10.1016/j.margeo.2004.03.011

Urban, N. R., Bayley, S. E., & Eisenreich, S. J. (1989). Export of dissolved organic carbon and acidity from peatlands. *Water Resources Research*, *25*(7), 1619–1628. https://doi.org/10.1029/WR025i007p01619

Urban, N. R., Verry, E. S., Eisenreich, S. J., Grigal, D. F., & Sebestyen, S. D. (2011). Nutrient cycling in upland/peatland watersheds. In R. K. Kolka, S. D. Sebestyen, E. S. Verry, & K. N. Brooks (Eds.), *Peatland biogeochemistry and watershed hydrology at the Marcell experimental forest* (pp. 213–241). CRC Press.

Van Bellen, S., Dallaire, P. L., Garneau, M., & Bergeron, Y. (2011). Quantifying spatial and temporal Holocene carbon accumulation in ombrotrophic peatlands of the Eastmain region, Quebec, Canada. *Global Biogeochemical Cycles*, *25*(2). https://doi.org/10.1029/2010gb003877

Van Bellen, S., Garneau, M., & Booth, R. K. (2011). Holocene carbon accumulation rates from three ombrotrophic peatlands in boreal Quebec, Canada: Impact of climate-driven ecohydrological change. *The Holocene*, *21*(8), 1217–1231. https://doi.org/10.1177/0959683611405243

Verry, E. S., Boelter, D. H., Päivänen, J., Nichols, D. S., Malterer, T. J., & Gafni, A. (2011). Physical properties of organic soils. In R. K. Kolka, S. D. Sebestyen, E. S. Verry, & K. N. Brooks (Eds.), *Peatland biogeochemistry and watershed hydrology at the Marcell experimental forest* (pp. 135–176). CRC Press. https://doi.org/10.1201/b10708-6

Verry, E. S., Brooks, K. N., Nichols, D. S., Ferris, D. R., & Sebestyen, S. D. (2011). Watershed hydrology. In R. K. Kolka, S. D. Sebestyen, E. S. Verry, & K. N. Brooks (Eds.), *Peatland biogeochemistry and watershed hydrology at the Marcell experimental forest* (pp. 193–212). CRC Press.

Visser, A., Broers, H. P., Purtschert, R., Sültenfuß, J., & de Jonge, M. (2013). Groundwater age distributions at a public drinking water supply well field derived from multiple age tracers (85Kr, 3H/3He, and 39Ar). *Water Research Research*, *41*(11), 7778–7796. https://doi.org/10.1002/2013WR014012

Visser, A., Moran, J. E., Hillegonds, D., Singleton, M. J., Kulongoski, J. T., Belitz, K., & Esser, B. K. (2016). Geostatistical analysis of tritium, groundwater age and other noble gas derived parameters in California. *Water Research*, *91*, 314–330. https://doi.org/10.1016/j.watres.2016.01.004

Whiticar, M. J. (1999). Carbon and hydrogen isotope systematics of bacterial formation and oxidation of methane. *Chemical Geology*, *161*(1–3), 291–314. https://doi.org/10.1016/s0009-2541(99)00092-3

Whitworth, K. L., Baldwin, D. S., & Kerr, J. L. (2014). The effect of temperature on leaching and subsequent decomposition of dissolved carbon from inundated floodplain litter: Implications for the generation of hypoxic blackwater in lowland floodplain rivers. *Chemistry and Ecology*, *30*(6), 491–500. https://doi.org/10.1080/02757540.2014.885019

Wilson, R. M., Fitzhugh, L., Whiting, G. J., Frolking, S., Harrison, M. D., Dimova, N., et al. (2017). Greenhouse gas balance over thaw-freeze cycles in discontinuous zone permafrost. *Journal of Geophysical Research: Biogeosciences*, *122*(2), 387–404. https://doi.org/10.1002/2016jg003600

Wilson, R. M., Hopple, A. M., Tfaily, M. M., Sebestyen, S. D., Schadt, C. W., Pfeifer-Meister, L., et al. (2016). Stability of peatland carbon to rising temperatures. *Nature Communications*, *7*(1), 1–10. https://doi.org/10.1038/ncomms13723

Wilson, R. M., Tfaily, M. M., Kolton, M., Johnson, E. R., Petro, C., Zalman, C. A., et al. (2021). Soil metabolome response to whole-ecosystem warming at the Spruce and Peatland Responses under changing environments experiment. *Proceedings of the National Academy of Sciences*, *118*(25), e2004192118. https://doi.org/10.1073/pnas.2004192118

Wilson, R. M., Tfaily, M. M., Rich, V. I., Keller, J. K., Bridgham, S. D., Zalman, C. M., et al. (2017). Hydrogenation of organic matter as a terminal electron sink sustains high CO_2: CH_4 production ratios during anaerobic decomposition. *Organic Geochemistry*, *112*, 22–32. https://doi.org/10.1016/j.orggeochem.2017.06.011

Yu, Z. C. (2012). Northern peatland carbon stocks and dynamics: A review. *Biogeosciences*, *9*(10), 4071–4085. https://doi.org/10.5194/bg-9-4071-2012

Yu, Z. C., Loisel, J., Brosseau, D. P., Beilman, D. W., & Hunt, S. J. (2010). Global peatland dynamics since the last glacial maximum. *Geophysical Research Letters*, *37*(13). https://doi.org/10.1029/2010gl043584

Zalman, C., Keller, J. K., Tfaily, M. M., Kolton, M., Pfeifer-Meister, L., Wilson, R. M., et al. (2018). Small differences in ombrotrophy control regional-scale variation in methane cycling among Sphagnum-dominated peatlands. *Biogeochemistry*, *139*, 155–177. https://doi.org/10.1007/s10533-018-0460-z